

Anomalous fluctuations of renewal-reward processes with heavy-tailed distributions

Hiroshi Horii,¹ Raphaël Lefevre,¹ Masato Itami,² and Takahiro Nemoto³

¹*Université de Paris, Laboratoire de Probabilités, Statistiques et Modélisation, UMR 8001, F-75205 Paris, France*

²*Center for Science Adventure and Collaborative Research Advancement, Kyoto University, Kyoto 606-8502, Japan*

³*Graduate School of Informatics, Kyoto University, Yoshida Hon-machi, Sakyo-ku, Kyoto, 606-8501, Japan*

For renewal-reward processes with a power-law decaying waiting time distribution, anomalously large probabilities are assigned to atypical values of the asymptotic processes. Previous works have revealed that this anomalous scaling causes a singularity in the corresponding large deviation function. In order to further understand this problem, we study in this article the scaling of variance in several renewal-reward processes: counting processes with two different power-law decaying waiting time distributions and a Knudsen gas (a heat conduction model). Through analytical and numerical analyses of these models, we find that the variances show an anomalous scaling when the exponent of the power law is -3 . For a counting process with the power-law exponent smaller than -3 , this anomalous scaling does not take place: this indicates that the processes only fluctuate around the expectation with an error that is compatible with a standard large deviation scaling. In this case, we argue that anomalous scaling appears in higher order cumulants. Finally, many-body particles interacting through soft-core interactions with the boundary conditions employed in the Knudsen gas are studied using numerical simulations. We observe that the variance scaling becomes normal even though the power-law exponent in the boundary conditions is -3 .

I. INTRODUCTION

A renewal-reward process, a generalisation of continuous time Markov processes, is one of the simplest stochastic processes that can describe random sequences with memory effects [1–3]. In contrast to its the Markov counterpart, in renewal-reward processes, the waiting time to move from one state to the next one can be distributed by a non-exponential function. The process can thus describe a broad spectrum of phenomena in physics [4] and other fields, including a melt up of the stock market [5, 6] and a super spreader in epidemics [7, 8], where memory effects are known to be important.

When the waiting time distribution has a power law, the dynamics show a slow convergence to its stationary states due to its heavy tail. For example, the probability that the state of the system always stays in the initial state during the dynamics remains non-negligible in the large time limit [9]. This anomalous behaviour can be characterised using a large deviation principle (LDP) [10, 11]. LDP states that the logarithmic probability of a time-averaged quantity is proportional with the averaging time (with a negative proportional constant), except for the trivial probability where the time averaged quantity takes its expectation. In renewal reward processes with power-law waiting time distributions, this proportional constant, known as a rate function or large deviation function (LDF), can take the value 0 not only for the expectation but also for a certain range of the values [9, 12, 13]. This indicates that these events are *more* likely to occur than in standard systems. We call this range of LDF taking the value 0

the affine part.

The affine part tells us that these rare events occur more likely than usual, but does not tell us how likely they do. To solve this problem, finite-time analyses of the LDP are necessary. One such attempt could be a so-called strong LDP, where the next order corrections of the logarithmic probability from the LDP are computed [14]. However, at present, it is not clear how this general theory can be extended to the case with the affine part. In [15], Tsirelson studied a renewal-reward process with general waiting time distributions and derived the next order correction to the LDP. But he used a condition in which an affine part can not be present. Recently, in [16], the authors studied finite-time corrections of the moment generating function under the condition that the affine part appears (Theorem 2.1). Yet they did not succeed to translate it to the correction term of the LDP.

In this article, instead of focusing on the probability of rare events, we focus on the variance of the time-averaged quantities. The variance can tell us directly how much the averaged quantities fluctuate. If one considers an exponential function for the waiting time distribution, the variance of the time-averaged quantity decreases proportionally to the inverse of the averaging time because this corresponds to the case of a process having a short memory. This indicates that the averaged value mostly falls in the range around the expectation with an error that is proportional with the inverse square root of the averaging time. In the presence of the affine part when heavy-tailed distributions are used for the waiting times, we identify, in this article, a

condition under which this scaling of the variance changes. This is consistent with the fact that heavy-tailed distributions introduce memory effects. Interestingly, not every power-law decaying distribution will result in this scaling modification of the variance: We show that for distributions whose density decay faster than $1/t^3$, the variance keeps its normal scaling. In that case, we expect that the scaling of higher order cumulants are affected, as discussed at the end of this article.

This article is organised as follows. Two models defined using renewal-reward processes are considered in this article: a counting process and a single particle model of heat conduction. These models are studied in Section II (counting process) and in Section III (heat conduction). Each section is organised with (i) a model introduction, (ii) introduction of renewal equations (a key tool to study the asymptotics of moments), (iii) analyses on the first moment, (iv) analyses on the second moment and variance, and (v) numerical studies. In Section IV, we discuss the scaling in higher order cumulants and how the scaling will change in more general heat-conduction systems. In particular, we observe that when several particles are present and interact through soft-core interactions, the time-average of physical quantities recover a “normal” behaviour. This seems to indicate that interactions break the strong memory effects that are present in the system of non-interacting particles.

II. COUNTING PROCESS

A. Model

A renewal-reward process is a model to describe events that occur sequentially. For a given event, the next event occurs after a random waiting time (also called a renewal time or arrival time). The waiting times are independent-and-identically distributed random positive variables $(\tau_k)_{k \in \mathbb{N}}$ with a probability density p . For this density, we consider the inverse Rayleigh distribution

$$p_\beta(\tau) = \frac{\beta}{\tau^3} \exp\left(-\frac{\beta}{2\tau^2}\right) \mathbf{1}(\tau > 0), \quad (1)$$

and the Pareto distribution

$$p_\alpha(\tau) = \frac{\alpha - 1}{(1 + \tau)^\alpha} \mathbf{1}(\tau > 0) \quad (2)$$

with $\alpha = 3$, both of which do not have a finite second moment, *i.e.*, $\mathbb{E}[\tau^2] = \infty$. The main quantity of interest in this section is the number of events that have occurred up to time $t > 0$. This is the counting

process N_t

$$N_t = \sup\{k : S_k \leq t\}, \quad (3)$$

where $S_k = \tau_1 + \dots + \tau_k$. We denote its q -th order moment by $m_q(t)$:

$$m_q(t) := \mathbb{E}[N_t^q]. \quad (4)$$

Note that with respect to [17], we consider the case where the expectation of the waiting time is finite and the renewal theorem [1] implies that the counting process N_t behaves as $N_t \sim t/\mathbb{E}[\tau]$ for $t \rightarrow \infty$. We study the fluctuations around that behaviour.

B. Renewal equations

To analyse the asymptotics of $m_q(t)$, we rely on renewal equations: a powerful tool to analyse renewal-reward processes. From a straightforward computation, one can establish the following renewal equation for $m_1(t)$ [2]:

$$m_1(t) = F(t) + \int_0^t ds m_1(t-s)p(s), \quad (5)$$

where F is the cumulative waiting time distribution function. From this equation, a simple expression for the Laplace transform of $m_1(t)$ is derived. Defining the Laplace transform of a function f by

$$\tilde{f}(s) := \int_0^\infty e^{-st} f(t) dt, \quad (6)$$

we then derive, from the equation (5),

$$\tilde{m}_1(s) = \frac{\tilde{F}(s)}{1 - s\tilde{F}(s)}, \quad (7)$$

where we have used $\tilde{p}(s) = s\tilde{F}(s)$.

Similarly, one can also derive a renewal equation for $m_2(t)$,

$$m_2(t) = \int_0^t \mathbb{E}[N_{t-s}^2] p(s) ds + 2 \int_0^t m_1(t-s)p(s) ds + F(t), \quad (8)$$

from which the Laplace transform of $m_2(t)$ is obtained as

$$\tilde{m}_2(s) = \tilde{m}_1(s)(1 + 2s\tilde{m}_1(s)). \quad (9)$$

Moreover, a renewal equation for the moment-generating function can be derived. (See Appendix A). From the equation, we derive the Laplace

transform of $m_q(t)$ as

$$\tilde{m}_q(s) = \sum_{k=1}^q \left[\sum_{i=1}^k \binom{k}{i} i^q (-1)^{k-i} \right] s^{k-1} [\tilde{m}_1(s)]^k. \quad (10)$$

C. Convergence of the first moment

When a waiting-time density p has a finite mean $\mathbb{E}[\tau] = \mu$ and a finite variance σ^2 , Feller has proven (Chapter 11, section 3, theorem 1) [3] that

$$\frac{m_1(t)}{t} - \frac{1}{\mu} \sim \frac{\sigma^2 - \mu^2}{2\mu^2 t}. \quad (11)$$

This result can be easily derived by using the following expansion:

$$s\tilde{F}(s) = 1 - \mu s + (\sigma^2 + \mu^2) \frac{s^2}{2} + o(s^2). \quad (12)$$

Indeed, by inserting it into (7), we get

$$\tilde{m}_1(s) = \frac{1}{\mu s^2} + \frac{\sigma^2 - \mu^2}{2\mu^2 s} + o\left(\frac{1}{s}\right), \quad (13)$$

which leads to

$$m_1(t) = \frac{1}{\mu} t + \frac{\sigma^2 - \mu^2}{2\mu^2} + o(1). \quad (14)$$

A rigorous justification to derive (14) from (13) is based on the Tauberian theorem [3]. See Appendix B for more details. From this argument, we can see that the condition $\mathbb{E}[\tau^2] = \infty$ is necessary for $m_1(t)$ to have an anomalous scaling. For this reason, we study in this section the two waiting-time distributions behaving at infinity like $1/t^3$.

Let us first consider the case of the inverse Rayleigh distribution. Let

$$\phi(s) = \int_0^\infty e^{-st} e^{-\frac{1}{2t^2}} dt. \quad (15)$$

We then have for its cumulative distribution function,

$$\tilde{F}_\beta(s) = \beta^{\frac{1}{2}} \phi(\beta^{\frac{1}{2}} s), \quad (16)$$

and

$$\tilde{m}_1(s) = \frac{\beta^{\frac{1}{2}} \phi(\beta^{\frac{1}{2}} s)}{1 - s\beta^{\frac{1}{2}} \phi(\beta^{\frac{1}{2}} s)}, \quad (17)$$

from (7). We then expand $\phi(s)$ in s :

$$\phi(s) = \frac{1}{s} - \sqrt{\frac{\pi}{2}} - \frac{1}{2} s \ln(s) + O(s), \quad (18)$$

leading to

$$\tilde{m}_1(s) = \sqrt{\frac{2}{\beta\pi}} \frac{1}{s^2} - \frac{1}{\pi s} \ln(s) + o\left(\frac{\ln(s)}{s}\right). \quad (19)$$

By using the Tauberian theorem (Appendix B), we obtain

$$\frac{m_1(t)}{t} - \sqrt{\frac{2}{\beta\pi}} = \frac{\ln(t)}{t\pi} + o\left(\frac{\ln(t)}{t}\right), \quad (20)$$

for large t . This is to be compared to (11): we see that the convergence is slower in our case.

We can repeat the same analysis in the case of the Pareto distribution. The cumulative distribution is derived as

$$F_3(t) := \mathbb{P}[\tau \leq t] = \begin{cases} 0 & t \leq 0 \\ 1 - \frac{1}{(1+t)^2} & t > 0. \end{cases} \quad (21)$$

when $m = 3$. We insert the Laplace transform of F_3 in (7) and again look at the expansion around s of \tilde{m} and get

$$\tilde{m}_1(s) = \frac{1}{s^2} - \frac{\ln(s)}{s} + o\left(\frac{\ln(s)}{s}\right). \quad (22)$$

We thus obtain the following behaviour for $m(t)$ for large t :

$$\frac{m_1(t)}{t} - 1 = \frac{\ln(t)}{t} + o\left(\frac{\ln(t)}{t}\right). \quad (23)$$

D. Convergence of the variance

We then study the large time behaviour of the variance

$$c_2(t) = \frac{m_2(t) - m_1(t)^2}{t^2}. \quad (24)$$

In the case that a waiting time density p has a finite mean $\mathbb{E}[\tau] = \mu$ and a finite variance σ^2 , we obtain from (9) and (13)

$$\tilde{m}_2(s) = \frac{2}{\mu^2 s^3} + \frac{1}{s^2} \frac{1}{\mu} \left(\frac{2\sigma^2 - \mu^2}{\mu^2} \right) + o\left(\frac{1}{s^2}\right), \quad (25)$$

which yields

$$m_2(t) = \frac{1}{\mu^2} t^2 + \frac{1}{\mu} \left(\frac{2\sigma^2 - \mu^2}{\mu^2} \right) t + o(t) \quad (26)$$

with the aid of the Tauberian theorem (B1). $c_2(t)$ is finally obtained as

$$c_2(t) = \frac{\sigma^2}{\mu^3 t} + o\left(\frac{1}{t}\right). \quad (27)$$

Let us now consider the case of the inverse Rayleigh distribution. Inserting the expression (19) for $\tilde{m}_1(s)$ in (9), we obtain,

$$\tilde{m}_2(s) = \frac{4}{\beta\pi} \frac{1}{s^3} - \frac{4\sqrt{2}}{\sqrt{\beta\pi^{3/2}}} \frac{\ln s}{s^2} + o\left(\frac{\ln(s)}{s^2}\right), \quad (28)$$

and then

$$m_2(t) = \frac{2}{\beta\pi} t^2 + \frac{4\sqrt{2}}{\sqrt{\beta\pi^{3/2}}} t \ln(t) + o(t \ln(t)). \quad (29)$$

Therefore

$$c_2(t) = \frac{2\sqrt{2}}{\sqrt{\beta\pi^{3/2}}} \frac{\ln(t)}{t} + o\left(\frac{\ln(t)}{t}\right). \quad (30)$$

Proceeding in the same way for the Pareto distribution, we obtain in that case

$$c_2(t) = 2 \frac{\ln t}{t} + o\left(\frac{\ln(t)}{t}\right). \quad (31)$$

E. Numerical study

We perform numerical simulations of the counting process N_t to illustrate the accuracy of (20), (23), (30) and (31). First, $m_1(t) - t\sqrt{2/(\beta\pi)}$ (resp. $m_1(t) - t$) computed from the numerical simulations is plotted as an orange line in Fig.1(a) (resp. Fig.1(b)) for the inverse Rayleigh (resp. Pareto) waiting time distribution. According to (20) and (23), these lines are equivalent to $\ln(t)/\pi + o(\ln(t))$ and $\ln(t) + o(\ln(t))$. Assuming that these $o(\ln(t))$ terms are constant over time when t is large, we next plot $\ln(t)/\pi + \text{const.}$ (Fig.1(a)) and $\ln(t) + \text{const.}$ (Fig.1(b)) in the same figures.

We then plot $(m_2(t) - m_1(t)^2)/t$ computed from the same numerical simulations in Fig.1 (c,d) for the inverse Rayleigh (Fig.1(c)) and the Pareto (Fig.1(d)) waiting time distributions. Reference lines $\frac{2\sqrt{2}}{\sqrt{\beta\pi^{3/2}}} \ln(t) + \text{const.}$ (Fig.1(c)) and $2 \ln(t) + \text{const.}$ (Fig.1(d)) are also plotted in the same figures. In these four figures, we observe good agreements between the slopes of the reference lines and the results of numerical simulations in semi-log scale. This demonstrates the validity of (20), (23), (30) and (31).

III. A PARTICLE CONFINED BETWEEN TWO HOT WALLS

Our aim in this section is to show that the slow convergence of the renewal function of processes having density $\sim 1/t^3$ as $t \rightarrow \infty$ also holds for physical

observables in a Knudsen gas [18]. For this, let us consider the model of a single particle bouncing back between two thermal walls.

A. Model

We consider a particle in a one-dimensional box that has two different temperatures at both ends. The confined tracer moves freely in the box of size 1 and is reflected at the end of the box with a random speed v distributed according to the following Rayleigh distribution:

$$q_{\beta_{\pm}}(v) = \beta_{\pm} v e^{-\beta_{\pm} \frac{v^2}{2}} \mathbb{1}(v > 0), \quad (32)$$

where $\beta_+ = 1/T_+$ (resp. $\beta_- = 1/T_-$) is the inverse temperature of the right (resp. left) wall.

Let $x_0 \in [0, 1]$ and v_0 the initial position and velocity of the particle and $\sigma_0 = v_0/|v_0|$. We denote the initial condition by θ , *i.e.*, $\theta = (x_0, v_0)$. The first time that the particle hits a wall is given by $S_{\theta,0} = (\frac{1}{2}(\sigma_0 + 1) - x_0)/v_0$, and the subsequent hitting times are given by

$$S_{\theta,k} = S_{\theta,0} + 1/v_1 + \dots + 1/v_k, \quad k \geq 1, \quad (33)$$

where v_k is a random variable distributed according to a law $q_{\beta_{\sigma_k}}$ and $\sigma_k = (-1)^k \sigma_0$. This may be rewritten as

$$S_{\theta,k} = S_{\theta,0} + \tau_1 + \dots + \tau_k, \quad k \geq 1 \quad (34)$$

with the sequence of independent waiting times $(\tau_k)_{k \in \mathbb{N}}$ distributed with the inverse Rayleigh distribution $p_{\beta_k}(\tau)$ defined as (1). The energy exchanged between the two walls during a time interval $[0, t]$ is defined as

$$J_{\theta}(t) := \frac{1}{2} \sum_{k=1}^{N_t} v_k^2 \sigma_k, \quad (35)$$

if $t \geq S_0^{\theta}$ and $J_{\theta}(t) = 0$ otherwise, where N_t is the counting process (3). We denote by $m_{\theta,q}(t)$ the q -th moment of $J_{\theta}(t)$:

$$m_{\theta,q}(t) = \mathbb{E}[J_{\theta}^q(t)]. \quad (36)$$

A generalisation to the system with an arbitrary box size L is straightforward. Indeed, denoting by $S_{\theta,k}^L$ the corresponding hitting times with the boundaries, it is easy to see that $S_{\theta,k}^L = L S_{\theta,k}^1$. This indicates that $N_t^L = N_{t/L}^1$ where N_t^L denotes the counting process corresponding to the hitting times $S_{\theta,k}^L$. For the energy current in a box of size L , we also have that

$$J_{\theta}^L(t) = J_{\theta}^1\left(\frac{t}{L}\right). \quad (37)$$

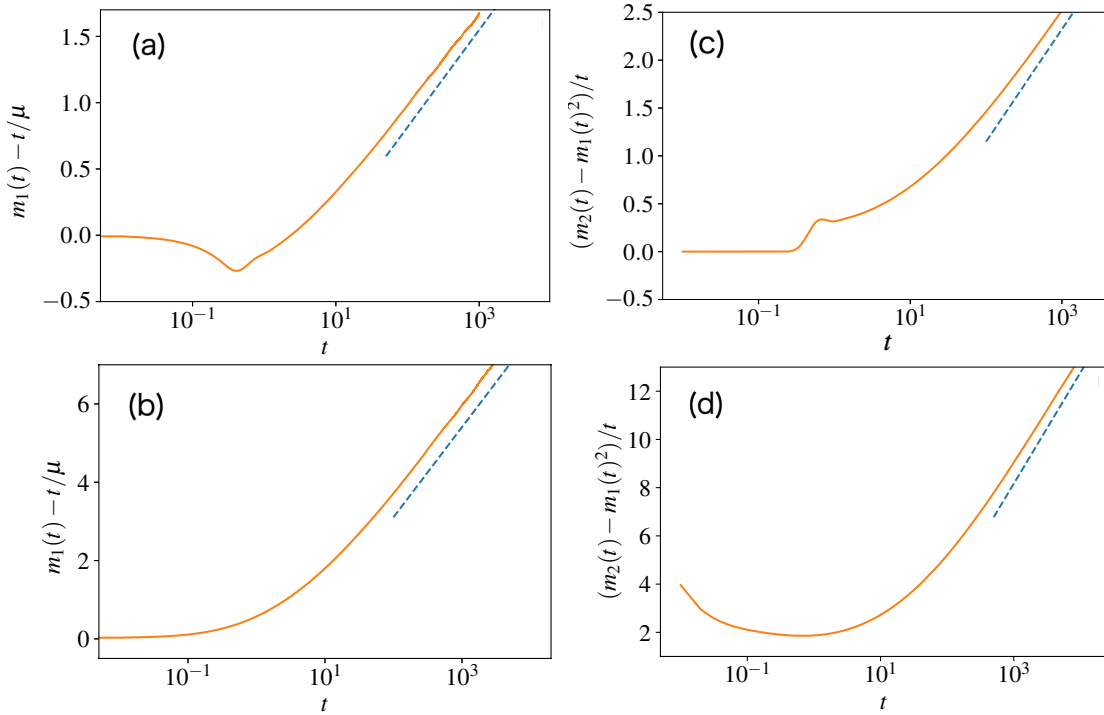


Fig. 1. **(a,b)** $m_1(t) - t/\mu$ obtained from numerical simulations of the counting process N_t (with 10^8 samples) are plotted as a function of time in log-scale as orange lines. For the inverse Rayleigh waiting time distribution (a), $\beta = 1$ and $\mu = 1/\sqrt{2}/(\beta\pi)$, while for the Pareto waiting time distribution (b), $m = 3$ and $\mu = 1$. $\ln(t)/\pi + \text{const.}$ and $\ln(t) + \text{const.}$ are also plotted as blue dashed lines for (a) and (b). **(c,d)** $(m_2(t) - m_1(t)^2)/t$ obtained from the same numerical simulations are plotted as a function of time as orange lines for the inverse Rayleigh waiting time distribution (c) and for the Pareto waiting time distribution (d). $\frac{2\sqrt{2}}{\sqrt{\beta\pi^{3/2}}}\ln(t) + \text{const.}$ for (c) and $2\ln(t) + \text{const.}$ for (d) are also plotted as blue dashed lines in the same figures. The agreements between the slopes of orange lines and those of blue lines in these semi-log graphs demonstrate the validity of (20), (23), (30) and (31), as detailed in the main text.

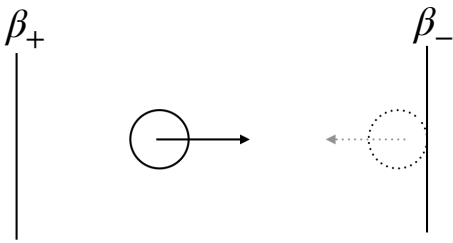


Fig. 2. Schematic figure to explain the setup of the 1 particle model. When the particle moves to the right (resp. left) wall, $\sigma_k = 1$ (resp. -1)

In the following we perform all computations with the case $L = 1$ and then obtain the result for an arbitrary $L > 0$ by using this scaling relation.

B. Convergence of the current: first moment

For simplicity, we consider only the following two types of initial conditions:

$$\theta_+ = (0, v_0) \quad (38)$$

with $v_0 < 0$ and

$$\theta_- = (1, v_0) \quad (39)$$

with $v_0 > 0$, *i.e.*, the cases of a particle just before hitting the left wall (temperature β_+) and of a particle just before hitting the right wall (inverse temperature β_-). As the particle immediately hits each wall when the process starts, the value of the initial velocity v_0 is unimportant. We thus denote by $+$ the initial condition θ_+ and by $-$ the initial condition θ_- .

Dynamics with these two initial conditions are related via the renewal property:

$$\mathbb{E}[J_{\pm}(t) \mid \tau_1 = u] = \frac{\pm 1}{2u^2} + \mathbb{E}[J_{\mp}(t-u)], \quad (40)$$

if $0 \leq u \leq t$ and $\mathbb{E}[J_{\pm}(t) \mid \tau_1 = u] = 0$ if $u > t$. This means that the process conditioned by the first-waiting time (the left-hand side) is equal to the other process with some increments (the right-hand side). By integrating (40) with respect to the inverse Rayleigh waiting time density (1), we obtain the following coupled renewal-reward equations for the currents

$$m_{-,1}(t) = - \left(\frac{1}{2t^2} + \frac{1}{\beta_-} \right) e^{-\frac{\beta_-}{2t^2}} + \int_0^t du m_{+,1}(t-u) p_{\beta_-}(u), \quad (41)$$

$$m_{+,1}(t) = + \left(\frac{1}{2t^2} + \frac{1}{\beta_+} \right) e^{-\frac{\beta_+}{2t^2}} + \int_0^t du m_{-,1}(t-u) p_{\beta_+}(u). \quad (42)$$

In order to derive the speed of convergence of the current, we perform a Laplace transform of (41) and (42):

$$\tilde{m}_{-,1}(s) = -\tilde{H}_-(s) - \frac{1}{\beta_-} \tilde{F}_{\beta_-}(s) + s \tilde{m}_{+,1}(s) \tilde{F}_{\beta_-}(s), \quad (43)$$

$$\tilde{m}_{+,1}(s) = \tilde{H}_+(s) + \frac{1}{\beta_+} \tilde{F}_{\beta_+}(s) + s \tilde{m}_{-,1}(s) \tilde{F}_{\beta_+}(s), \quad (44)$$

where $\tilde{H}_{\pm}(s)$ is the Laplace transform of $H_{\pm}(t) = \frac{1}{2t^2} e^{-\frac{\beta_{\pm}}{2t^2}}$ and $\tilde{F}_{\beta_{\pm}}(s)$ is the Laplace transform of the cumulative inverse Rayleigh distribution. By substituting (43) into (44), we then obtain an equation for $\tilde{m}_{+,1}(s)$ as

$$\tilde{m}_{+,1}(s) = \frac{\tilde{H}_+(s) + \frac{1}{\beta_+} \tilde{F}_{\beta_+}(s)}{1 - s^2 \tilde{F}_{\beta_+}(s) \tilde{F}_{\beta_-}(s)} - s \tilde{F}_{\beta_+}(s) \frac{\tilde{H}_-(s) + \frac{1}{\beta_-} \tilde{F}_{\beta_-}(s)}{1 - s^2 \tilde{F}_{\beta_+}(s) \tilde{F}_{\beta_-}(s)}, \quad (45)$$

which leads to

$$\tilde{m}_{\pm,1}(s) = \kappa \left(\frac{1}{\beta_+} - \frac{1}{\beta_-} \right) \frac{1}{s^2} - \kappa^2 \frac{(\beta_+ + \beta_-)}{2} \left(\frac{1}{\beta_+} - \frac{1}{\beta_-} \right) \frac{\ln(s)}{s} + o\left(\frac{\ln(s)}{s}\right), \quad (46)$$

where κ is the conductivity given by

$$\kappa^{-1} = \left(\frac{\pi\beta_-}{2} \right)^{\frac{1}{2}} + \left(\frac{\pi\beta_+}{2} \right)^{\frac{1}{2}}. \quad (47)$$

Using again the Tauberian theorem for Laplace transform (Appendix B), we finally get,

$$\frac{m_{\pm,1}(t)}{t} = \kappa \left(\frac{1}{\beta_+} - \frac{1}{\beta_-} \right) + \kappa^2 \frac{(\beta_+ + \beta_-)}{2} \left(\frac{1}{\beta_+} - \frac{1}{\beta_-} \right) \frac{\ln t}{t} + o\left(\frac{\ln(t)}{t}\right). \quad (48)$$

Note that the asymptotic form of the average current $m_{+,1}(t)$ and $m_{-,1}(t)$ have opposite signs, but this is because the definition of the current includes $(-1)^{\pm 1}$ term: these two expressions are physical equivalent. For the average current in a box of size L , we get

$$\begin{aligned} \frac{m_{\pm,1}^L(t)}{t} &= \frac{1}{L} \frac{m_{\pm,1}^1\left(\frac{t}{L}\right)}{\frac{t}{L}} \\ &= \frac{\kappa}{L} \left(\frac{1}{\beta_+} - \frac{1}{\beta_-} \right) + \kappa^2 \frac{(\beta_+ + \beta_-)}{2} \left(\frac{1}{\beta_+} - \frac{1}{\beta_-} \right) \frac{\ln(t)}{t} + o\left(\frac{\ln(t)}{t}\right). \end{aligned} \quad (49)$$

C. Variance of the current of energy between heat baths

We next discuss the large time asymptotics of the variance of the current. The renewal property for the second moment of the current is expressed by

$$\mathbb{E}[J_{\pm}^2(t) \mid \tau_1 = u] = \left[\frac{1}{2u^2} \right]^2 + \frac{\sigma}{u^2} \mathbb{E}[J_{\mp}(t-u)] + \mathbb{E}[J_{\mp}^2(t-u)] \quad (50)$$

if $0 \leq u \leq t$ and $\mathbb{E}[J_{\pm}(t) \mid \tau_1 = u] = 0$ if $u > t$. Let us introduce for $t > 0$,

$$L_{\pm}(t) = \left(\frac{1}{4t^4} + \frac{1}{\beta_{\pm} t^2} + \frac{2}{\beta_{\pm}^2} \right) e^{-\frac{\beta_{\pm}}{2t^2}},$$

$$g_{\pm}(t) = \frac{\beta_{\pm}}{t^5} e^{-\frac{\beta_{\pm}}{2t^2}}.$$

Then, integrating (50) with respect to the inverse Rayleigh waiting time density (1) and using the relation

$$\int_0^t du \frac{1}{4u^4} p_{\beta_{\pm}}(u) = \left(\frac{1}{4t^4} + \frac{1}{\beta_{\pm} t^2} + \frac{2}{\beta_{\pm}^2} \right) e^{-\frac{\beta_{\pm}}{2t^2}} \quad (51)$$

for $t > 0$, the renewal equations for the second moment of the current are derived as

$$m_{+,2}(t) = L_+(t) + \int_0^t du m_{-,1}(t-u)g_+(u) + \int_0^t du m_{-,2}(t-u)p_{\beta_+}(u), \quad (52)$$

$$m_{-,2}(t) = L_-(t) - \int_0^t du m_{+,1}(t-u)g_-(u) + \int_0^t du m_{+,2}(t-u)p_{\beta_-}(u), \quad (53)$$

In order to derive the large time asymptotic of the second moment of the current, we perform Laplace transform of (52) and (53),

$$\tilde{m}_{+,2}(s) = \tilde{L}_+(s) + \tilde{m}_{-,1}(s)\tilde{g}_+(s) + s\tilde{m}_{-,2}(s)\tilde{F}_{\beta_+}(s), \quad (54)$$

$$\tilde{m}_{-,2}(s) = \tilde{L}_-(s) - \tilde{m}_{+,1}(s)\tilde{g}_-(s) + s\tilde{m}_{+,2}(s)\tilde{F}_{\beta_-}(s). \quad (55)$$

We solve these linear equations for $\tilde{m}_{-,2}(s)$ and $\tilde{m}_{+,2}(s)$ by using $\tilde{m}_{\pm,1}(s)$ obtained in section III B and the following expansions of $\tilde{L}_{\pm}(s)$ and $\tilde{g}_{\pm}(s)$

$$\tilde{L}_{\pm}(s) = \frac{2}{\beta_{\pm}^2 s} - \frac{3}{4\beta_{\pm}^{3/2}}\sqrt{\frac{\pi}{2}} + \frac{s}{4\beta_{\pm}} + O(s^2), \quad (56)$$

$$\tilde{g}_{\pm}(s) = \frac{2}{\beta_{\pm}} - \frac{1}{\sqrt{\beta_{\pm}}}\sqrt{\frac{\pi}{2}}s + O(s^2). \quad (57)$$

Recalling $\tilde{F}_{\beta_{\pm}}(s) = \beta_{\pm}^{\frac{1}{2}}\phi(\beta_{\pm}^{\frac{1}{2}}s)$ with

$$\phi(s) = \frac{1}{s} - \sqrt{\frac{\pi}{2}} - \frac{1}{2}s \ln(s) + O(s), \quad (58)$$

the Laplace transform of the second moment of the current is derived as

$$\begin{aligned} \tilde{m}_{\pm,2}(s) &= 2\kappa^2 \left(\frac{1}{\beta_+} - \frac{1}{\beta_-} \right)^2 \frac{1}{s^3} \\ &\quad - \frac{2\kappa^3 \ln(s)}{s^2} (\beta_+ + \beta_-) \left(\frac{1}{\beta_+} - \frac{1}{\beta_-} \right)^2 \\ &\quad + o\left(\frac{\ln(s)}{s^2}\right). \end{aligned} \quad (59)$$

From the Tauberian theorem (Appendix B), we finally arrive at the asymptotic form of the variance

$$\begin{aligned} \text{Var}\left(\frac{J_{\pm}(t)}{t}\right) &= \frac{m_{\pm,2}(t)}{t^2} - \frac{(m_{\pm,1}(t))^2}{t^2} \\ &= \kappa^3 (\beta_+ + \beta_-) \left(\frac{1}{\beta_+} - \frac{1}{\beta_-} \right)^2 \frac{\ln(t)}{t} \\ &\quad + o\left(\frac{\ln(t)}{t}\right). \end{aligned} \quad (60)$$

This result agrees with our previous work [12]. As for the variance of the current in a box of size L , we get:

$$\begin{aligned} \text{Var}\left(\frac{J_{\pm}^L(t)}{t}\right) &= \frac{1}{L^2} \text{Var}\left(\frac{J_{\pm}^1(\frac{t}{L})}{t/L}\right) \\ &= \frac{1}{L} \kappa^3 (\beta_+ + \beta_-) \left(\frac{1}{\beta_+} - \frac{1}{\beta_-} \right)^2 \frac{\ln(t)}{t} \\ &\quad + o\left(\frac{\ln(t)}{t}\right). \end{aligned} \quad (61)$$

D. Convergence of the thermal energy

A similar formulation can be applied to study the convergence of the time-averaged kinetic energy defined as

$$E_{\pm}(t) = \frac{1}{2} \sum_{k=1}^{N_t} \frac{1}{\tau_k}. \quad (62)$$

The expected values of the energy are denoted by

$$m_E^{\pm}(t) = \mathbb{E}[E_{\pm}(t)]. \quad (63)$$

As in the section III B, we construct two equations in Laplace space

$$\tilde{m}_E^+(s) = \tilde{h}_+(s) + \tilde{g}_+(s) + s\tilde{m}_E^-(s)\tilde{F}_{\beta_+}(s), \quad (64)$$

$$\tilde{m}_E^-(s) = \tilde{h}_-(s) + \tilde{g}_-(s) + s\tilde{m}_E^+(s)\tilde{F}_{\beta_-}(s), \quad (65)$$

Here, $h(t)$ and $g(t)$ are given by

$$h_{\pm}(t) = \frac{e^{-\frac{\beta_{\pm}}{2t^2}}}{2t}, \quad (66)$$

$$g_{\pm}(t) = \frac{1}{2} \sqrt{\frac{\pi}{2\beta_{\pm}}} \text{Erfc}\left[\sqrt{\frac{\beta_{\pm}}{2}} \frac{1}{t}\right]. \quad (67)$$

Thus, $\tilde{m}_E^+(s)$ is calculated as

$$\begin{aligned} \tilde{m}_E^+(s) &= \frac{\tilde{h}_+(s) + \tilde{g}_+(s)}{1 - s^2 \tilde{F}_{\beta_+}(s) \tilde{F}_{\beta_-}(s)} \\ &\quad + s \tilde{F}_{\beta_+}(s) \frac{\tilde{h}_-(s) + \tilde{g}_-(s)}{1 - s^2 \tilde{F}_{\beta_+}(s) \tilde{F}_{\beta_-}(s)}. \end{aligned} \quad (68)$$

Proceeding in the same way as for the current, we can expand the functions involved for small s and obtain

$$\begin{aligned} \tilde{m}_E^+(s) &= \sqrt{\frac{\pi}{8}} \kappa \left(\sqrt{\frac{1}{\beta_+}} + \sqrt{\frac{1}{\beta_-}} \right) \frac{1}{s^2} - \frac{1}{4} \sqrt{\frac{\pi}{2}} \kappa^2 (\beta_+ \\ &\quad + \beta_-) \left(\sqrt{\frac{1}{\beta_+}} + \sqrt{\frac{1}{\beta_-}} \right) \frac{\ln(s)}{s} + o\left(\frac{\ln(s)}{s}\right). \end{aligned} \quad (69)$$

As with the derivation of (48), the large time asymptotics of $m_E^\pm(t)$ are derived as

$$\begin{aligned}
m_E(t) &= \sqrt{\frac{\pi}{8}} \kappa \left(\sqrt{\frac{1}{\beta_+}} + \sqrt{\frac{1}{\beta_-}} \right) t \\
&\quad + \frac{1}{4} \sqrt{\frac{\pi}{2}} \kappa^2 (\beta_+ + \beta_-) \left(\sqrt{\frac{1}{\beta_+}} + \sqrt{\frac{1}{\beta_-}} \right) \ln(t) \\
&\quad + o(\ln(t)).
\end{aligned} \tag{70}$$

E. Numerical simulations

We numerically simulate the one-particle model to check the validity of (48) and (60). We estimate $m_{+,1}(t)$ and $m_{+,2}(t)$ from the numerical simulations, and plot $m_{+,1}(t) - \kappa(1/\beta_+ - 1/\beta_-)$ and $m_{\pm,2}(t)/t^2 - (m_{\pm,1}(t))^2/t^2$ in Fig. 3 (a,b). In the same figures, we also plot $(\kappa^2/2)(\beta_+ + \beta_-)(1/\beta_+ - 1/\beta_-)(\ln t)/t + \text{const.}$ and $\kappa^3(\beta_+ + \beta_-)(1/\beta_+ - 1/\beta_-)^2 + \text{const.}$ as blue dashed lines. We observe that the slopes of the orange lines in semi-log scale asymptotically converge to those of blue dashed lines. This demonstrates (48) and (60).

IV. DISCUSSION

A. A counting process with smaller power-law exponents

In the first part of this article, we studied a counting process N_t with two heavy-tail waiting time distributions: the Pareto distribution with $\alpha = 3$ and the inverse Rayleigh distribution. These two waiting time distributions have an asymptotic form $1/\tau^3$ when the waiting time τ is large, implying that the variance of the waiting time $\mathbb{E}[\tau^2]$ diverges. Because of this divergence, we discussed that the scaled variance $c_2(t)t$ of the counting process N_t also diverges in the large t limit. We indeed derived that it is asymptotically proportional with $\ln(t)$, diverging as $t \rightarrow \infty$.

A natural question would be, can we get a similar result with a waiting time distribution that has an asymptotic form $1/\tau^\alpha$ with $\alpha > 3$? As demonstrated in Appendix A, one can formulate a general framework, for the Pareto distribution, to derive analytical expressions of the Laplace transform of $\mathbb{E}[N_t^k]$ ($k = 1, 2, 3, \dots$) for any α . As an example, we computed the first, second and third moments for $\alpha = 4$, from which we show the third cumulant of N_t/t has an asymptotic form $\ln(t)/t^2$ when t is large. This indicates that the third-order cumulant multiplied by

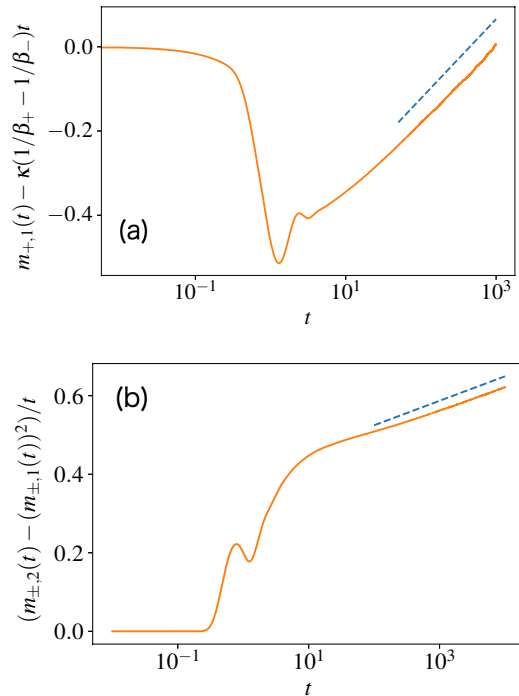


Fig. 3. $m_{+,1}(t) - \kappa(1/\beta_+ - 1/\beta_-)$ (a) and $m_{\pm,2}(t)/t^2 - (m_{\pm,1}(t))^2/t^2$ (b) obtained from numerical simulations (with 10^8 samples) are plotted as orange lines. $\beta_+ = 1$, $\beta_- = 2$. Blue dashed lines are $(\kappa^2/2)(\beta_+ + \beta_-)(1/\beta_+ - 1/\beta_-)(\ln t)/t + \text{const.}$ and $\kappa^3(\beta_+ + \beta_-)(1/\beta_+ - 1/\beta_-)^2 + \text{const.}$ The slopes of the numerical-simulation results in semi-log scale converge to those of the dashed reference lines, showing the validity of (48) and (60).

t^2 is asymptotically proportional with $\ln(t)$, which is also diverging in the large t limit.

For the counting process with a general fat tail waiting time distribution (that has a power law decay as $t \rightarrow \infty$), an existence of the affine part in the scaled cumulant generating function (sCGF) $G(s) = \lim_{t \rightarrow \infty} (1/t) \ln \mathbb{E}[e^{sN_t}]$ has been proven [16]. When the sCGF is analytic, it can be expanded using scaled cumulants \bar{c}_i ($i = 1, 2, \dots$) as $G(s) = \sum_{i=1}^{\infty} (\bar{c}_i/i!) s^i$ by definition, where \bar{c}_i is defined as $\lim_{t \rightarrow \infty} c_i t^{i-1}$ with the i -th order cumulant c_i of N_t/t . In the presence of the affine part, sCGF is not analytic, implying that some scaled cumulants $\lim_{t \rightarrow \infty} c_i t^{i-1}$ diverge. Based on the observation above, we conjecture that the k -th order scaled cumulant converges when $k < \alpha - 2$. When $k = \alpha - 2$, the k -th order cumulant c_i increases proportionally with $\ln(t)/t^{i-1}$, resulting in $\ln(t)$ divergence of $\lim_{t \rightarrow \infty} c_i t^{i-1}$. It is an interesting future work to study this conjecture.

B. Many particles confined in the two hot walls

In the second part of this article, we studied a particle confined in the two walls in different temperatures, and observed that the scaled variance diverges proportionally with $\ln(t)$. Here we discuss if we can observe the same divergence in many-body particles confined in the walls.

One-dimensional hard-core interacting particles exchange their velocities when they collide. The dynamics of these particles can thus be exactly mapped to the dynamics of non-interacting many-body particles. Let $J_\infty^{\mathcal{N},L,D}(t)$ and $J_0^{\mathcal{N},L,D}(t)$ be the energy currents of \mathcal{N} hard-core interacting and non-interacting particles of diameter D confined in a one-dimensional box of size L , respectively. Then, we get

$$\mathbb{E} \left[\frac{J_\infty^{\mathcal{N},L+\mathcal{N}D,D}(t)}{t} \right] = \mathbb{E} \left[\frac{J_0^{\mathcal{N},L+D,D}(t)}{t} \right] \quad (71)$$

$$= \mathcal{N} \frac{m_{\pm,1}^L(t)}{t}, \quad (72)$$

$$\text{Var} \left(\frac{J_\infty^{\mathcal{N},L+\mathcal{N}D,D}(t)}{t} \right) = \text{Var} \left(\frac{J_0^{\mathcal{N},L+D,D}(t)}{t} \right) \quad (73)$$

$$= \mathcal{N} \text{Var} \left(\frac{J_\pm^L(t)}{t} \right), \quad (74)$$


where $m_{\pm,1}^L(t)$ and $\text{Var}(J_\pm^L(t)/t)$ are given in Eqs. (49) and (61), respectively. This implies that the logarithmic divergence of the scaled variance should be observed in hard-core interacting systems. In soft-core interacting systems, on the other hand, the same mapping cannot be used. This is because of the collisions involving more than two particles, where the exchange rule of velocities no longer holds. To demonstrate this insight, we have performed simulations of hard-core and soft-core interacting particles. The details of the simulations are explained in Appendix C, and the results are shown in Fig. 4, where $J_{\text{MD}}(t)$ is the total energy transferred to the colder wall from time 0 to t , and k is a parameter corresponding to the softness of particles. Note that $k = \infty$ corresponds to the case of the hard-core interacting system. We observed that the $\ln(t)$ divergence disappears as soon as particles start to interact via soft-core interactions. It is an interesting future problem to develop a framework to quantitatively understand the disappearance of the divergence in soft-core particles.

C. Related studies

Finally, we list related studies. Studying a variance in a process that is defined with power-law decaying distribution is not something new. In [17], several anomalous diffusion models were studied using continuous-time random walk, and revealed anomalous scaling in their diffusion coefficients. These anomalous scalings were argued to be universally observed in transports in random media [4]. One of the authors also studied a single big jump principle, which states that the sum of random variables can be approximated by their maximum when the probability distribution of the variables has a power-law [19].

Singularities of large deviation functions of time-cumulative quantities are also known as dynamical phase transitions, and have been studied in many physical models, such as glass formers [20–26], lattice gas models [27–33], diffusive hydrodynamic equations [34–36], and high-dimensional chaotic dynamics [37–39] and active matters [40–43]. Finite-size scalings of the large deviation functions have been performed in several works (see an interesting recent work [44] for example), but variance scalings have not been intensively studied in this field yet.

ACKNOWLEDGMENTS

The authors thank S. Sasa for useful comments. H.H. is in the Cofund MathInParis PhD project that has received funding from the European Union's Horizon 2020 research and innovation programme under the Marie Skłodowska-Curie grant agreement No. 754362 . R.L. is supported by the ANR-15-CE40-0020-01 grant LSD. This work was supported by JSPS KAKENHI under Grants No. JP17H01148 and No. JP20J00003.

Appendix A: k -th moment of a counting process with heavy-tailed distributions

Here, we derive the k -th moment of a counting process N_t (with a waiting time density p) by using a renewal equation. The moment-generating function $M_h(t)$ is defined by

$$M_h(t) \equiv \mathbb{E} [e^{hN_t}]. \quad (\text{A1})$$

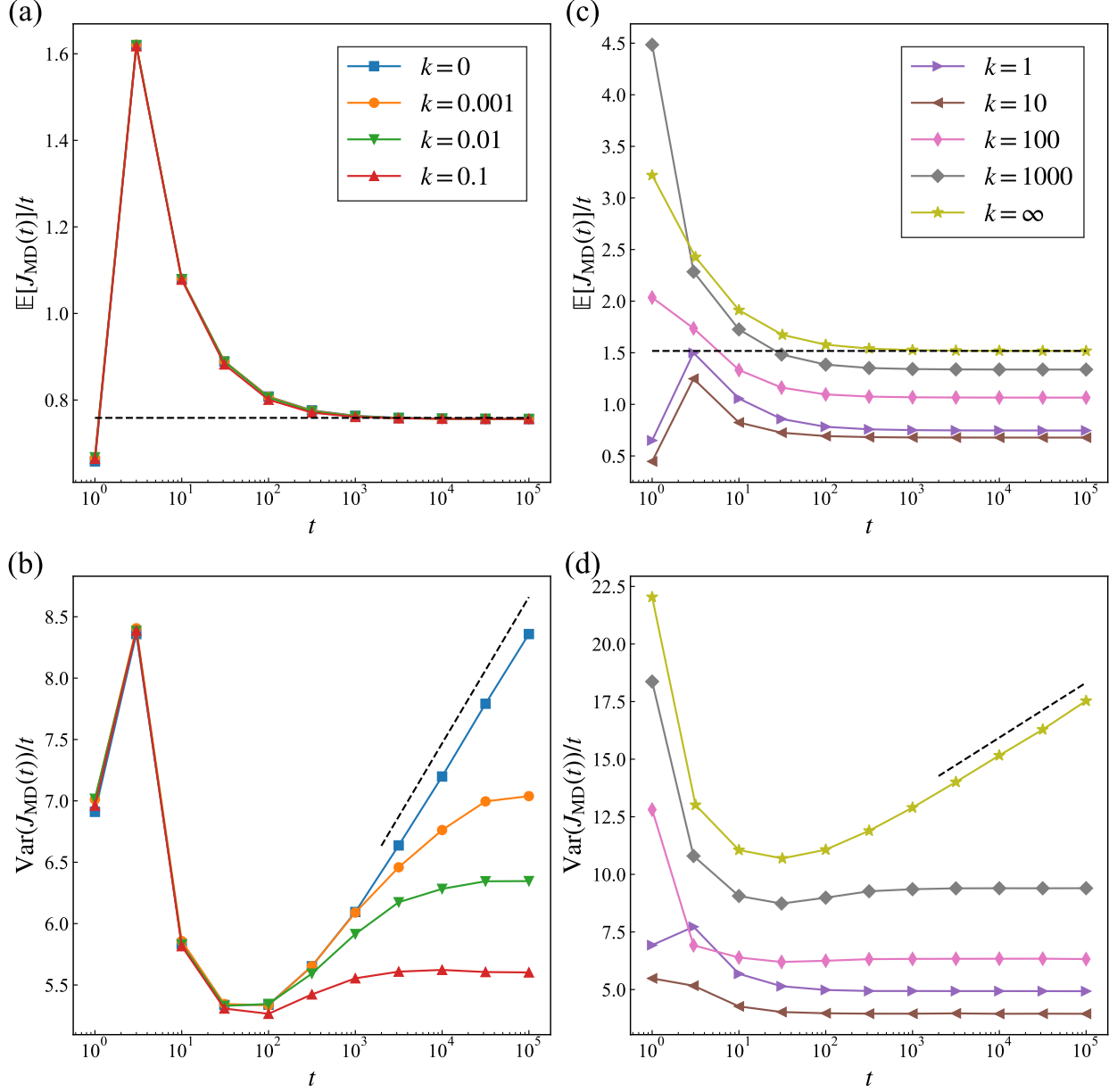


Fig. 4. Statistical properties of $J_{\text{MD}}(t)$ over time for different particle softnesses averaged over 10^6 samples when $\mathcal{N} = 3$, $D = 1$, $L = 5$, $\beta_+ = 1/3$, and $\beta_- = 1$. (a) $\mathbb{E}[J_{\text{MD}}(t)]/t$ versus t for $k = 0, 0.001, 0.01$, and 0.1 . The dashed line is $\mathbb{E}[J_{\text{MD}}(t)]/t = \mathcal{N}\kappa(\beta_+^{-1} - \beta_-^{-1})/(L - D)$. (b) $\text{Var}(J_{\text{MD}}(t))/t$ versus t for $k = 0, 0.001, 0.01$, and 0.1 . The dashed line is $\text{Var}(J_{\text{MD}}(t))/t = \mathcal{N}\kappa^3(\beta_+ + \beta_-)(\beta_+^{-1} - \beta_-^{-1})^2 \ln(t)/(L - D) + \text{const.}$ (c) $\mathbb{E}[J_{\text{MD}}(t)]/t$ versus t for $k = 1, 10, 100, 1000$, and ∞ . The dashed line is $\mathbb{E}[J_{\text{MD}}(t)]/t = \mathcal{N}\kappa(\beta_+^{-1} - \beta_-^{-1})/(L - \mathcal{N}D)$. (d) $\text{Var}(J_{\text{MD}}(t))/t$ versus t for $k = 1, 10, 100, 1000$, and ∞ . The dashed line is $\text{Var}(J_{\text{MD}}(t))/t = \mathcal{N}\kappa^3(\beta_+ + \beta_-)(\beta_+^{-1} - \beta_-^{-1})^2 \ln(t)/(L - \mathcal{N}D) + \text{const.}$

Using

$$\begin{aligned}
 \mathbb{E}[e^{hN_t}] &= \int_0^\infty du \mathbb{E}[e^{hN_t} | \tau_1 = u] p(u) \\
 &= \int_0^t du \mathbb{E}[e^{h(N_t - u + 1)}] p(u) \\
 &\quad + \int_t^\infty du p(u), \tag{A2}
 \end{aligned}$$

we obtain the following renewal equation

$$M_h(t) = e^h \int_0^t du M_h(t - u) p(u) + \int_t^\infty du p(u). \tag{A3}$$

The Laplace transform of this equation gives

$$\tilde{M}_h(s) = e^h \tilde{M}_h(s) \tilde{p}(s) + \frac{1 - \tilde{p}(s)}{s}, \quad (\text{A4})$$

which leads to

$$\tilde{M}_h(s) = \frac{1}{s} \frac{1 - \tilde{p}(s)}{1 - \tilde{p}(s)e^h}. \quad (\text{A5})$$

Using

$$\tilde{m}_1(s) = \frac{\tilde{p}(s)}{s(1 - \tilde{p}(s))}, \quad (\text{A6})$$

we can rewrite (A5) as

$$\begin{aligned} \tilde{M}_h(s) &= \frac{1}{s} \frac{1}{1 - s\tilde{m}_1(s)(e^h - 1)} \\ &= \sum_{q=0}^{\infty} (e^h - 1)^q s^{q-1} [\tilde{m}_1(s)]^q. \end{aligned} \quad (\text{A7})$$

Because

$$\lim_{h \rightarrow 0} \frac{d^k}{dh^k} (e^h - 1)^q = \sum_{i=0}^q \binom{q}{i} i^k (-1)^{q-i}, \quad (\text{A8})$$

$$\lim_{h \rightarrow 0} \frac{d^k}{dh^k} (e^h - 1)^q = 0, \quad \text{for } k < q, \quad (\text{A9})$$

and

$$\lim_{h \rightarrow 0} \frac{d^k}{dh^k} \tilde{M}_h(s) = \tilde{m}_k(s), \quad (\text{A10})$$

we have

$$\tilde{m}_k(s) = \sum_{q=1}^k \left[\sum_{i=1}^q \binom{q}{i} i^k (-1)^{q-i} \right] s^{q-1} [\tilde{m}_1(s)]^q. \quad (\text{A11})$$

Let us now consider the Pareto distribution (2) with $\alpha = 4$ as the waiting time density. In this case, we have

$$\tilde{m}_1(s) = \frac{2}{s^2} + \frac{1}{s} + o\left(\frac{1}{s}\right), \quad (\text{A12})$$

$$\tilde{m}_2(s) = \frac{8}{s^3} + \frac{10}{s^2} + \frac{16 \ln(s)}{s} + o\left(\frac{\ln(s)}{s}\right), \quad (\text{A13})$$

$$\begin{aligned} \tilde{m}_3(s) &= \tilde{m}_1(s) + 6s\tilde{m}_1^2(s) + 6s^2\tilde{m}_1^3(s) \\ &= \frac{48}{s^4} + \frac{96}{s^3} + \frac{144 \ln(s)}{s^2} + o\left(\frac{\ln(s)}{s^2}\right) \end{aligned} \quad (\text{A14})$$

from (A11) for large s . Using the following inverse Laplace transform

$$\int_0^{\infty} e^{-st} \ln(t) dt = \left(-\frac{\ln(s) + \gamma}{s} \right), \quad (\text{A15})$$

we calculate the inverse Laplace transform of $\tilde{m}_k(s)$ as

$$m_1(t) \sim 2t + 1, \quad (\text{A16})$$

$$m_2(t) \sim 4t^2 + 10t - 16 \ln(t), \quad (\text{A17})$$

$$m_3(t) \sim 8t^3 + 48t^2 + 206t - 144t \ln(t) \quad (\text{A18})$$

as $t \rightarrow \infty$. The second cumulants c_2 defined as (24) and the third cumulant c_3 (defined as the third cumulant of N_t/t^3) are then given by

$$c_2(t) = \frac{6}{t} + o\left(\frac{1}{t}\right), \quad (\text{A19})$$

$$\begin{aligned} c_3(t) &= \frac{m_3(t) - 3m_1(t)m_2(t) + 2m_1^3(t)}{t^3} \\ &= -\frac{48 \ln(t)}{t^2} + o\left(\frac{\ln(t)}{t^2}\right). \end{aligned} \quad (\text{A20})$$

Appendix B: Tauberian theorem

The Tauberian theorem is stated in [3] Ch.XIII.5, theorem 4. In our context it can be stated as follows. If the Laplace transform \tilde{m} of the renewal function m satisfies

$$\tilde{m}(s) \sim \frac{1}{s^\rho} L\left(\frac{1}{s}\right), \quad s \rightarrow 0$$

for some $\rho > 0$ and some slowly varying (*i.e.*, a function L is slowly varying if for any $x > 0$, $\lim_{t \rightarrow \infty} \frac{L(xt)}{L(t)} = 1$) function L then

$$m(t) \sim \frac{1}{\Gamma(\rho)} t^{\rho-1} L(t). \quad (\text{B1})$$

Appendix C: Simulation detail

\mathcal{N} particles of mass m and diameter D are lined up on a line $[0, L]$. Let (r_i, p_i) be the position and momentum of the i th particle. The total energy transferred to the right wall from time 0 to t is defined by

$$J_{\text{MD}}(t) = \sum_i \sum_{k_i} \left\{ \frac{|p_i(t_{k_i} - 0)|^2}{2m} - \frac{|p_i(t_{k_i} + 0)|^2}{2m} \right\} \quad (\text{C1})$$

with $0 \leq t_{k_i} \leq t$, where $t_{k_i} \pm 0$ is the time just before/after the i th particle collides with the right wall for the k_i th time.

For the case of the soft-core interacting system, a short-range interaction potential Φ between two

particles is given by

$$\Phi(|r_i - r_j|) = \frac{k}{2} (D - |r_i - r_j|)^2 \Theta(D - |r_i - r_j|), \quad (\text{C2})$$

where Θ is the Heaviside step function, and k is a parameter corresponding to the softness of particles. The boundary condition is the same as explained in Sec. III A. Using the second-order symplectic integrator, we numerically solved the equations of mo-

tion for the particles, and calculated $\mathbb{E}[J_{\text{MD}}(t)]$ and $\text{Var}(J_{\text{MD}}(t))$ for various values of k . In the simulation, we set the parameter values as $\mathcal{N} = 3$, $L = 5$, $m = D = 1$, $\beta_+ = 1/3$, and $\beta_- = 1$. The time-discretization step-size was set to 0.01.

For the case of the hard-core interacting system (denoted by $k = \infty$), we performed event-driven simulations in which two particles instantaneously exchange velocities when they come into contact. The boundary condition and the parameter values were the same as for the soft-core particle system.

-
- [1] Søren Asmussen. *Applied probability and queues* volume 51. Springer Science & Business Media 2008.
- [2] Geoffrey Grimmett and David Stirzaker. *Probability and random processes*. Oxford university press 2020.
- [3] William Feller. *An introduction to probability theory and its applications, vol 2*. John Wiley & Sons 2008.
- [4] Eli Barkai and Stanislav Burov. Packets of diffusing particles exhibit universal exponential tails. *Physical review letters* **124**, 060603 (2020).
- [5] Brendan O Bradley and Murad S Taqqu. Financial risk and heavy tails. In *Handbook of heavy tailed distributions in finance* pages 35. Elsevier 2003.
- [6] Paul Glasserman, Philip Heidelberger, and Perwez Shahabuddin. Portfolio value-at-risk with heavy-tailed risk factors. *Mathematical Finance* **12**, 239 (2002).
- [7] Felix Wong and James J Collins. Evidence that coronavirus superspreading is fat-tailed. *Proceedings of the National Academy of Sciences* **117**, 29416 (2020).
- [8] Anne Schneeberger, Catherine H Mercer, Simon AJ Gregson, Neil M Ferguson, Constance A Nyamukapa, Roy M Anderson, Anne M Johnson, and Geoff P Garnett. Scale-free networks and sexually transmitted diseases: a description of observed patterns of sexual contacts in Britain and Zimbabwe. *Sexually transmitted diseases* **31**, 380 (2004).
- [9] Raphaël Lefevre and Lorenzo Zambotti. Hot scatterers and tracers for the transfer of heat in collisional dynamics. *Journal of Statistical Physics* **139**, 686 (2010).
- [10] Hugo Touchette. The large deviation approach to statistical mechanics. *Physics Reports* **478**, 1 (2009).
- [11] Frank Den Hollander. *Large deviations* volume 14. American Mathematical Soc. 2008.
- [12] Raphael Lefevre, Mauro Mariani, and Lorenzo Zambotti. Large deviations of the current in stochastic collisional dynamics. *Journal of Mathematical Physics* **52**, 033302 (2011).
- [13] Raphaël Lefevre, Mauro Mariani, and Lorenzo Zambotti. Macroscopic fluctuation theory of aerogel dynamics. *Journal of Statistical Mechanics: Theory and Experiment* **2010**, L12004 (2010).
- [14] Cyrille Joutard. A strong large deviation theorem. *Mathematical Methods of Statistics* **22**, 155 (2013).
- [15] Boris Tsirelson. From uniform renewal theorem to uniform large and moderate deviations for renewal-reward processes. *Electronic Communications in Probability* **18**, 1 (2013).
- [16] Hiroshi Horii, Raphaël Lefevre, and Takahiro Nemoto. Large time asymptotic of heavy tailed renewal processes. *Journal of Statistical Physics* **186**, 1 (2022).
- [17] Ralf Metzler, Jae-Hyung Jeon, Andrey G Cherstvy, and Eli Barkai. Anomalous diffusion models and their properties: non-stationarity, non-ergodicity, and ageing at the centenary of single particle tracking. *Physical Chemistry Chemical Physics* **16**, 24128 (2014).
- [18] Joel L Lebowitz and Harry L Frisch. Model of nonequilibrium ensemble: Knudsen gas. *Physical Review* **107**, 917 (1957).
- [19] Alessandro Vezzani, Eli Barkai, and Raffaella Burioli. Single-big-jump principle in physical modeling. *Physical Review E* **100**, 012108 (2019).
- [20] Lester O Hedges, Robert L Jack, Juan P Garrahan, and David Chandler. Dynamic order-disorder in atomistic models of structural glass formers. *Science* **323**, 1309 (2009).
- [21] Juan P Garrahan, Robert L Jack, Vivien Lecomte, Estelle Pitard, Kristina van Duijvendijk, and Frédéric van Wijland. First-order dynamical phase transition in models of glasses: an approach based on ensembles of histories. *Journal of Physics A: Mathematical and Theoretical* **42**, 075007 (2009).
- [22] Robert L Jack and Peter Sollich. Large deviations and ensembles of trajectories in stochastic models. *Progress of Theoretical Physics Supplement* **184**, 304 (2010).
- [23] Estelle Pitard, Vivien Lecomte, and Frédéric Van Wijland. Dynamic transition in an atomic glass former: A molecular-dynamics evidence. *EPL (Europhysics Letters)* **96**, 56002 (2011).
- [24] David T Limmer and David Chandler. Theory of amorphous ices. *Proceedings of the National Academy of Sciences* **111**, 9413 (2014).
- [25] Takahiro Nemoto, Robert L Jack, and Vivien Lecomte. Finite-size scaling of a first-order dynamical phase transition: Adaptive population dynamics

- and an effective model. *Physical review letters* **118**, 115702 (2017).
- [26] Thomas Speck, Alex Malins, and C Patrick Royall. First-order phase transition in a model glass former: Coupling of local structure and dynamics. *Physical review letters* **109**, 195703 (2012).
- [27] Thierry Bodineau and Bernard Derrida. Distribution of current in nonequilibrium diffusive systems and phase transitions. *Physical Review E* **72**, 066110 (2005).
- [28] Cécile Appert-Rolland, Bernard Derrida, Vivien Lecomte, and Frédéric Van Wijland. Universal cumulants of the current in diffusive systems on a ring. *Physical Review E* **78**, 021122 (2008).
- [29] T Bodineau, B Derrida, V Lecomte, and F Van Wijland. Long range correlations and phase transitions in non-equilibrium diffusive systems. *Journal of Statistical Physics* **133**, 1013 (2008).
- [30] Thierry Bodineau, Vivien Lecomte, and Cristina Toninelli. Finite size scaling of the dynamical free-energy in a kinetically constrained model. *Journal of Statistical Physics* **147**, 1 (2012).
- [31] Yongjoo Baek, Yariv Kafri, and Vivien Lecomte. Dynamical symmetry breaking and phase transitions in driven diffusive systems. *Physical review letters* **118**, 030604 (2017).
- [32] Ohad Shpielberg. Geometrical interpretation of dynamical phase transitions in boundary-driven systems. *Physical Review E* **96**, 062108 (2017).
- [33] Ohad Shpielberg, Takahiro Nemoto, and João Caetano. Universality in dynamical phase transitions of diffusive systems. *Physical Review E* **98**, 052116 (2018).
- [34] Lorenzo Bertini, Alberto De Sole, Davide Gabrielli, Gianni Jona-Lasinio, and Claudio Landim. Current fluctuations in stochastic lattice gases. *Physical review letters* **94**, 030601 (2005).
- [35] Pablo I Hurtado and Pedro L Garrido. Spontaneous symmetry breaking at the fluctuating level. *Physical review letters* **107**, 180601 (2011).
- [36] N Tizón-Escamilla, PI Hurtado, and PL Garrido. Structure of the optimal path to a fluctuation. *Physical Review E* **95**, 032119 (2017).
- [37] Julien Tailleur and Jorge Kurchan. Probing rare physical trajectories with Lyapunov weighted dynamics. *Nature Physics* **3**, 203 (2007).
- [38] Tanguy Laffargue, Khanh-Dang Nguyen Thu Lam, Jorge Kurchan, and Julien Tailleur. Large deviations of Lyapunov exponents. *Journal of Physics A: Mathematical and Theoretical* **46**, 254002 (2013).
- [39] F Bouchet, C Nardini, and T Tangarife. Stochastic averaging, large deviations and random transitions for the dynamics of 2D and geostrophic turbulent vortices. *Fluid Dynamics Research* **46**, 061416 (2014).
- [40] Suriyanarayanan Vaikuntanathan, Todd R Gingrich, and Phillip L Geissler. Dynamic phase transitions in simple driven kinetic networks. *Physical Review E* **89**, 062108 (2014).
- [41] Francesco Cagnetta, Federico Corberi, Giuseppe Gonnella, and Antonio Suma. Large fluctuations and dynamic phase transition in a system of self-propelled particles. *Physical review letters* **119**, 158002 (2017).
- [42] Stephen Whitelam, Katherine Klymko, and Dibyendu Mandal. Phase separation and large deviations of lattice active matter. *The Journal of chemical physics* **148**, 154902 (2018).
- [43] Takahiro Nemoto, Étienne Fodor, Michael E Cates, Robert L Jack, and Julien Tailleur. Optimizing active work: Dynamical phase transitions, collective motion, and jamming. *Physical Review E* **99**, 022605 (2019).
- [44] Luke Causer, Mari Carmen Bañuls, and Juan P. Garrahan. Finite Time Large Deviations via Matrix Product States. *Phys. Rev. Lett.* **128**, 090605 (2022).